Spinal dural arteriovenous fistulas: evaluation with MR angiography.

B C Bowen, K Fraser, J P Kochan, P M Pattany, B A Green and R M Quencer

AJNR Am J Neuroradiol 1995, 16 (10) 2029-2043
http://www.ajnr.org/content/16/10/2029

Spinal Dural Arteriovenous Fistulas: Evaluation with MR Angiography

B. C. Bowen, K. Fraser, J. P. Kochan, P. M. Pattany, B. A. Green, and R. M. Quencer

PURPOSE: To show that postgadolinium three-dimensional time-of-flight MR angiography shows abnormal intradural vessels associated with spinal dural arteriovenous fistula better than routine MR imaging and provides screening information useful for subsequent diagnostic conventional angiography and/or posttreatment evaluation. **METHODS:** Precontrast and postcontrast MR imaging and MR angiograms, as well as subsequent digital subtraction angiograms, were obtained for eight patients with dural arteriorvenous fistulas, diagnosed with digital subtraction angiography and verified with surgery. In four patients, MR studies also were obtained after surgery. **RESULTS:** All patients had cord hyperintensity of T2-weighted images and postgadolinium enhancement on T1-weighted images. Five had vessellike signal abnormalities in the subarachnoid space on MR. Abnormal intradural vessels were detected in all eight patients with MR angiography. Comparison with digital subtraction angiography revealed these vessels to be primarily enlarged veins of the coronal venous plexus on the cord surface. In six patients, the medullary vein draining the fistula was demonstrated, indicating the level of the fistula, later identified by digital subtraction angiography. After surgical obliteration of the fistula, the draining medullary vein and most or all of the abnormal coronal veins were no longer demonstrated, with decrease or resolution of cord hyperintensity on T2-weighted images. **CONCLUSION:** Postgadolinium, spinal MR angiography in cases of suspected dural arteriovenous fistula provides information about intradural veins that supplements the diagnostic value of the MR imaging results, facilitates the subsequent digital subtraction angiography study, and, in treated cases, reflects the success of surgery and/or embolization.

Index terms: Fistula, arteriovenous; Fistula, spinal dural; Magnetic resonance angiography; Spinal angiography.

AJNR Am J Neuroradiol 16:2029–2043, November 1995

Compared with the large number of head and neck vascular studies, magnetic resonance (MR) angiography of spinal vascular lesions has received relatively little attention (1). One series (2) and a few isolated cases (3–5) of spinal vascular malformation demonstrated with phase contrast MR angiography have been reported. MR imaging alone of such lesions has been more thoroughly investigated, and spin-echo MR findings have been described (6–9). The MR imaging findings, though, are often not consistent or specific, and, in fact, supine myelography still is recommended by some investigators as the procedure of choice in screening for spinal dural arteriovenous fistula (AVF) before conventional angiography (Halbach VV et al, "Interventional Neuroradiology," presented at the 32nd Annual Meeting of the American Society of Neuroradiology, Nashville, Tenn, May 3–7, 1994). Digital subtraction angiography (DSA) is the standard of reference for diagnostic imaging of spinal vascular lesions (10). Based on the DSA appearance and surgical findings, spinal vascular malformations are generally, although not universally, classified as intradural (intramedullary and/or extramedullary) arteriovenous malformation (AVM) or fistula, and dural AVF (11–14). Recommended treatment of dural AVF consists of surgical obliteration (13, 15, 16) and/or embolization (12, 17, 18).

This study had three main goals: (*a*) to show, by way of comparison with conventional spinal

Received November 1, 1994; accepted after revision March 10, 1995.

From the Departments of Radiology (B.C.B., K.F., J.P.K., P.M.P., R.M.Q.) and Neurosurgery (B.A.G.), University of Miami (Fla) School of Medicine.

Address reprint requests to Dr Brian C. Bowen, Department of Radiology (R-308), MRI Center, 1115 NW 14th St, Miami, FL 33135.

AJNR 16:2029–2043, Nov 1995 0195-6108/95/1610–2029

angiograms, that three-dimensional time-of-flight MR angiography better demonstrates abnormal spinal vessels associated with dural AVF than routine spin-echo MR imaging; (*b*) to show that MR angiography often shows the major medullary vein(s) draining the fistula, thus helping to direct subsequent conventional angiography, and (*c*) to show that MR angiography may be used to assess the status of enlarged intradural veins after surgery for dural fistula.

Materials and Methods

Eight patients (45 to 71 years of age; mean, 60 years) with surgically proved spinal vascular malformation (see below) underwent MR imaging and MR angiography of the spine followed by selective spinal DSA. The clinical findings in these patients fit the characteristic picture described by Kendall, Logue, and colleagues (16, 19, 20). The presenting symptoms (duration, 4 months to 2 years) were progressive bilateral lower extremity weakness (7 of 8), pain (5 of 8), and numbness (5 of 8), as well as micturition disorder (6 of 8) and defecation disorder (3 of 8). On neurologic examination, the clinical signs were bilateral lower extremity weakness (7 of 8; all muscle groups, proximal more than distal in 2 of 8) and increased (5 of 8) or decreased (2 of 8) deep tendon reflexes, as well as extensor plantar responses (4 of 8). Sensory level (5 of 8) or decreased sensation to pin prick and/or light touch in a patchy distribution (3 of 8) was elicited.

MR imaging and angiography were performed using a 1.5-T scanner equipped with a quadrature radio frequency receive-only surface coil for spine imaging. T1-weighted sagittal and axial spin-echo images (700/16–20/1–2 [repetition time/echo time/excitations]), as well as T2-weighted spin-echo (2500/80/1) or gradient-echo (600/18/4; flip angle, 20°) sagittal images were acquired. Two patients referred from other hospitals had recent MR imaging that included fast spin-echo (4000/102/2, echo train length 16) sagittal scans. For time-of-flight MR angiography, a 3-D volume acquisition (single slab) with coronal or sagittal orientation encompassing the spinal canal was implemented using a radio frequency-spoiled gradient-echo pulse sequence (40–50/10; flip angle, 20°; 50 0.7- to 0.8-mm partitions, 256 × 180 matrix, 180-mm rectangular [230:256] field of view, 11-minute acquisition time, velocity compensation along all three coordinate directions). The spinal region evaluated with MR angiography was chosen on the basis of clinical neurologic deficits and the location of abnormalities on pregadolinium spin-echo MR images. Neither magnetization transfer suppression nor ramp pulses was used.

Spatial presaturation pulses were incorporated into the MR angiography pulse sequence. Presaturation was used to lessen aliasing and motion-induced artifacts. For 3-D slab acquisitions with coronal orientation, bilateral presaturation zones were used. These were each 10 cm wide and encompassed the flanks of the abdomen, lateral chest wall, and/or shoulders. The medial border of each slab was located at approximately one third to one half of the distance from the midline to the lateral chest or abdominal wall. For sagittal slab acquisitions, the presaturation zone encompassing the anterior abdomen and chest was 10 cm thick, whereas the presaturation zone posterior to the spine was approximately 2 to 3 cm, depending on the thickness needed to suppress signal from skin and subcutaneous fat.

T1-weighted spin-echo images and MR angiography source images (partitions) were acquired before and after intravenous administration of a gadolinium chelate, gadopentetate dimeglumine, at a dose of 0.15 to 0.2 mmol/kg. Manual infusion of gadolinium required approximately 1 minute, and acquisition of the MR angiographic source images was begun less than 1 minute after completion of the infusion. Postgadolinium coronal and sagittal 3-D data sets were acquired, followed by the T1-weighted images. Because two postgadolinium 3-D slabs were acquired, each requiring approximately 11 minutes, the higher gadolinium dose of 0.15 to 0.2 mmol/kg was used (21, 22). The time required to complete each patient's study was approximately 60 minutes. In some cases, the examination time was shortened by omitting the pregadolinium T1-weighted axial scan.

MR projection angiograms were produced with the commercially available, region-of-interest (targeted) maximum intensity projection algorithm. Spinal intradural vessels identified on these images were considered abnormal if three qualitative findings were present: (*a*) apparent vessel enlargement (based on ranges of vessel size given in Thron [23]); (*b*) marked tortuosity of these vessels; and (*c*) increased number of visible vessels. In healthy subjects, only the largest thoracolumbar segments of the anterior and posterior median veins, and sometimes the great medullary veins, are seen on postgadolinium images (Fig 1).

DSA was performed within 1 to 21 days of the MR examination. Segmental arteries were injected (300 psi) with iohexol (300 mg iodine per milliliter) at 1 mL/s. Biplane images with 1024 × 1024 matrix resolution (Neurostar system, Siemens, Erlangen, Germany) were obtained at a rate of 2 to 4 frames per second. Images were acquired for 25 seconds. The anterior spinal artery was identified in all cases.

Results

MR imaging findings in the cases of dural AVF were variable with respect to cord enlargement, signal characteristics on precontrast T1-weighted images, and detection of vessellike hypointensities in the subarachnoid space (Table). In all cases, there was confluent hyperintensity centrally within the cord on the T2-weighted images (Figs 2A and 3A). The location of the hyperintensity was variable with respect to the level of the fistula, being primarily

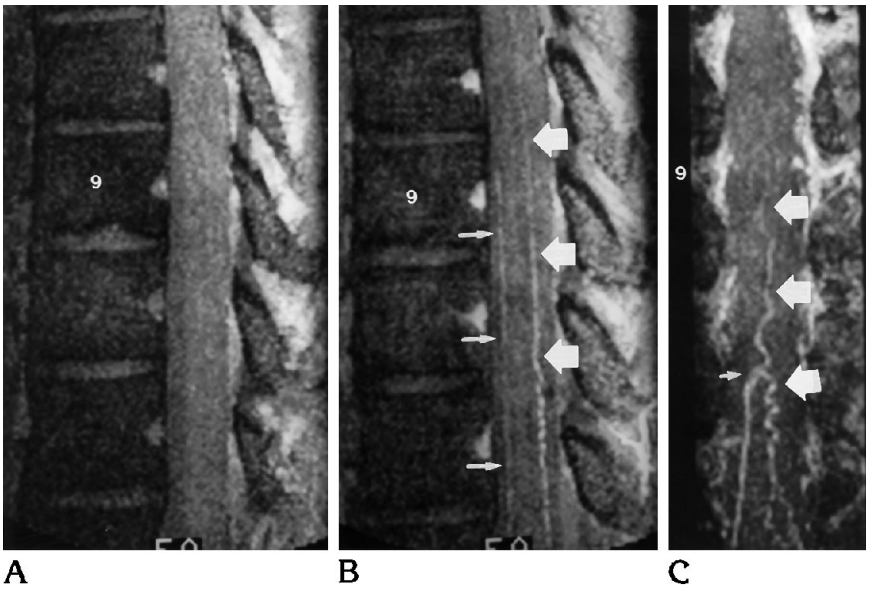

Fig 1. Normal MR angiography of the lower thoracic spine (T-6 to T-12) in a patient with normal spinal DSA findings.

A and *B*, Midsagittal, subvolume projection angiogram (5 source images) before (*A*) and after (*B*) intravenous administration of gadolinium. A midline intradural vessel (*large white arrows*) along the posterior aspect of the cord is demonstrated in B. This vessel corresponds in location to the posterior median vein. The vessel (*small white arrows*) corresponding to the anterior median vein has less signal and appears smaller.

C, Postgadolinium, coronal, subvolume angiogram encompassing the posterior half of the canal was reconstructed with data from the same acquisition as in B. The posterior median vein (*large white arrows*) is serpiginous without marked tortuousity. Although not visible above T-9 in C, this vein is detected up to T6-7 in B. A relatively straight vessel extending from the right side of the canal at T11–12 corresponds to a right T-12 great medullary vein. The anastomosis (*small white arrow*) with the posterior median vein has a "coat-hook" configuration, described on conventional angiography by Fried et al (28).

cephalad (patient 6, Fig 2A) or caudad (patient 7), yet usually involving about 5 vertebral levels, including the level of the fistula (patient 8, Fig 3A). Cord enhancement on the postgadolinium T1-weighted images (Figs 3C and 4A) also was detected in all cases.

On postgadolinium MR angiography, abnormal intradural vessels were identified in all cases (Table), appearing relatively large, very tortuous or convoluted, and numerous (Figs 2B, 2C, 3D, 3E, 4B, and 4C) in comparison with the normal straight or minimally serpiginous vessel on the posterior and/or anterior surface of the cord, in the midline (Figs 1B and C). Correlation with DSA images revealed that the large vessels corresponded to enlarged intradural veins, principally the anterior and posterior median spinal veins and veins of the coronal venous plexus located on the surface of the cord (Figs 2, 3, and 4).

In cases with little or no evidence of intradural hypervascularity on the spin-echo MR images (patients 1, 5, and 6 in the Table), the MR angiography source images and projection angiograms more convincingly demonstrated the enlarged intradural vessels resulting from the fistula (compare Fig 2A and B). These vessels were most prominent one or more vertebral levels above the fistula site (Fig 2B). In cases with vascular signal abnormalities apparent over several vertebral levels on the spin-echo images (patients 2, 3, 4, 7, and 8), the postgadolinium subvolume projection angiograms better demonstrated the continuity and extent (cephalocaudad and anteroposterior) of the enlarged intradural veins (compare Figs 3A–C to Fig 3D and 4A to 4B). In the evaluation of these patients, the region of interest for a subvolume angiogram was usually chosen so that only vessels in the posterior half, or in the anterior half, of the canal were displayed on a coronal image (Figs 1C, 2C, and 4C), and only the vessels within a few millimeters of the midline were displayed on a sagittal image (Figs 1B, 2B, 2G, and 4B). The hyperintense signal in the intradural vessels on these images was distinguishable from patchy or diffuse cord enhancement (Figs 3C and D).

In addition to showing abnormal intradural vessels extending over many spinal levels, postgadolinium MR angiography demonstrated a large vessel that coursed from the neural foramen where a fistula was located to the midline in 6 of 8 cases (Table). The course of this vessel, as displayed on targeted maximum intensity projection (MIP) images, corresponded to the course of the enlarged medullary vein draining the fistula, as shown on delayed DSA images (Figs 2D and 3F). Caudal to the anastomosis between the draining medullary vein

Spinal vascular malformations: MR and DSA findings

Patient	Age, y/Sex	MR Imaging					MR Angiography			DSA		
		Cord*				Subarachnoid Space†	Coronal Veins‡		Medullary Vein	Vascular Malformation§		
		Enlargement	T1-Weighted	T2-Weighted	Postgadolinium T1-Weighted	Vessels	Level	Cord Surface	Level	Type	Feeding Artery/ Medullary Vein	Early Veins
1	62/M	+	−	+	+	−	T8-T12	A>P	L T-10	1A	L T-10	A
2	56/M	+	−	+	+	+	T7-10	P>A	L T-11, T-12	1A	L T-12	A
							T10-12	A>P				
3	68/M	−	+	+	+	+	T4-6‖	A>P	Not shown	1A	R T-12	A
							T7-10	P>A				
4	50/M	−	−	+	+	+	T5-8	P	R T-6	1A	R T-5/R T-6	P
							T8-10	A>P				
5	71/F	+	−	+	+	−	T8-11	P>A	R T-8	1A	R T-8	P
6	65/M	−	−	+	+	−	T8-11	A>P	R T-12	1A	R T-12	P
							T11-12	P>A				
7	45/M	+	−	+	+	+	C6-T6‖	A>P	Not shown	1A	R T-8	P
							T7-T12	P≥A				
8	67/F	+	−	+	+	+	T5-7	A>P	R T-12	1A	R T-12	P
							T8-L1	P>A				

* MR imaging findings of cord enlargement, decreased signal intensity on T1-weighted images, enhancement on postgadolinium T1-weighted images, and increased signal intensity on T2-weighted images are indicated with a + when present and − when absent.

† The finding of multiple hypointense foci in the subarachnoid space on T2-weighted images, or scalloping of the cord contour on T1-weighted images, involving at least two vertebral levels is referred to as *vessels* and is indicated with a + when present.

‡ The extent (levels) of the tortous, enlarged vessels, primarily veins, traveling cephalocaudad along the cord surface (coronal veins), as demonstrated by MR angiography, is indicated. A>P, for example, refers to a predominance of vessels on the anterior (A) surface of the cord compared with the posterior (P) surface on the postgadolinium, midsagittal, subvolume projection MR angiogram.

§ Spinal vascular malformations are identified by type, based on the classification in Prince (21). Type 1A is a dural AVF with a single feeding artery (see "Discussion"). *Feeding artery* refers to the radiculomedullary-dural artery, and *medullary vein* to the vein draining the fistula for patients 1 through 8. The feeding artery and draining vein involved the same foramen, except in patient 4 in whom dural branches of the right T-5 artery supplied a malformation that was drained by the T-6 medullary vein.

‖ Abnormal coronal veins extended beyond the thoracic region, which was imaged with a single, coronal-slab MR angiogram.

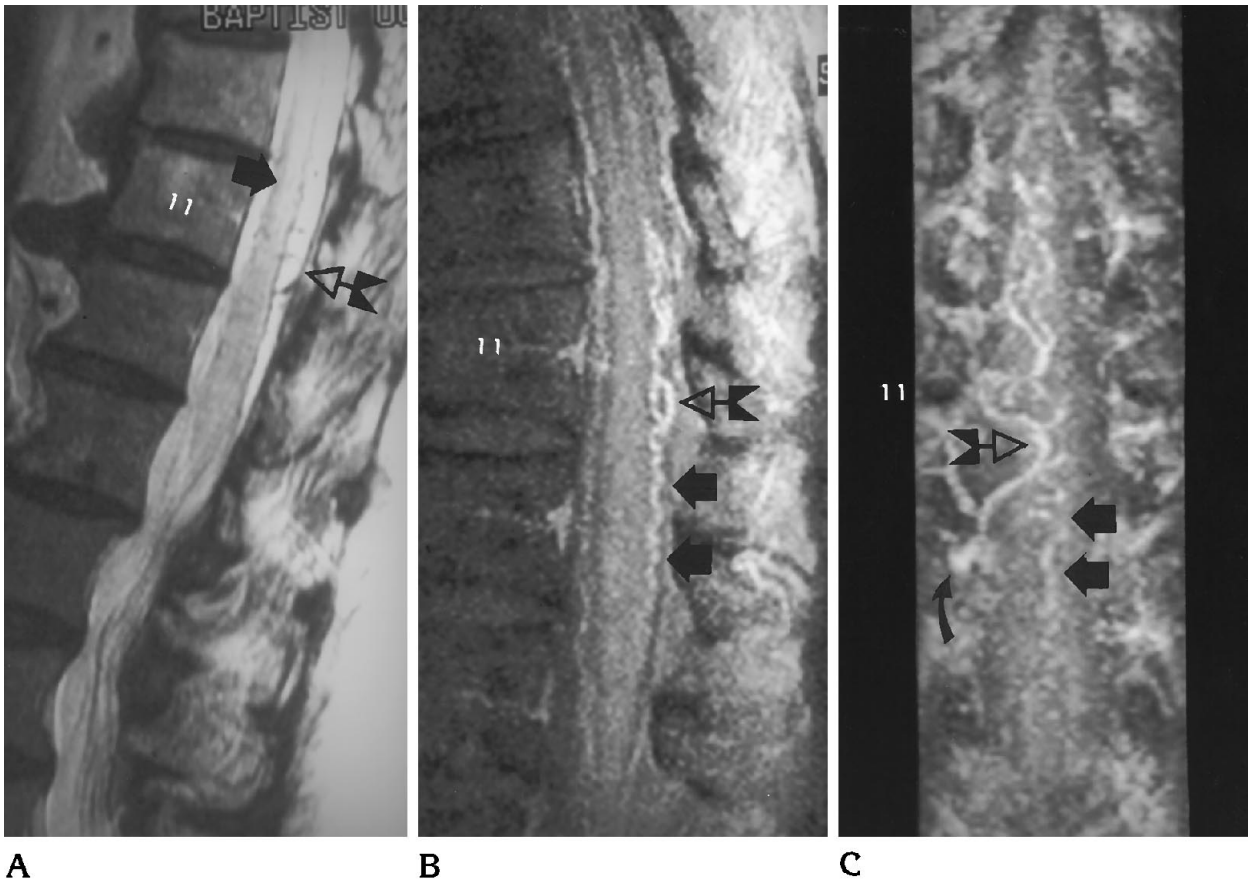

Fig 2. Right T-12 dural AVF (patient 6).

A, Midsagittal, T2-weighted, fast spin-echo image demonstrates central hyperintensity (*arrow*) in the lower thoracic cord. A few hypointense foci (*open arrow*) are located in the subarachnoid space posterior to the cord at T-11.

B, Postgadolinium, midsagittal, subvolume MR angiogram (T-9 to L-2). Markedly tortuous intradural vessels are present posterior and anterior to the cord, especially at T-11. A prominent vessel segment (*open arrow*) is located posteriorly at T-11. Anterior and inferior to this larger segment, the posterior median vein (*arrows*) courses inferiorly toward the conus tip at L1-2.

C, Coronal, subvolume MR angiogram, from the same acquisition as B. The subvolume image encompasses the posterior half of the canal. A relatively large and tortuous vessel extends toward the midline from an enhancing focus (*curved arrow*) in the right T-12 foramen. The curved midline segment (*open arrow*) is the same one visible posterior to the cord in B. The vessel then turns laterally toward the right side of the canal before returning again to the midline, where it anastomoses with additional tortuous vessels on the posterior surface of the cord. The posterior median vein at T-12 has a "question mark" configuration (*arrows*). *Figure continues.*

and the coronal veins, a single dominant midline vessel on the posterior surface of the conus was identified with MR angiography (Figs 2C, 3E, and 4C). This vessel corresponded to an enlarged, caudally draining posterior median vein, seen on delayed DSA images and at surgery (Figs 2D, 2E, 3F, 3H, and 4E).

A major difference between MR angiography and DSA was that intradural veins demonstrated on multiple sequential DSA images in temporal sequence appeared together on a single MIP image (Fig 4). As a result, some intradural vessels were better delineated on postgadolinium MR angiography than on the DSA images. For example, in patient 7, the anterior median vein was well seen on the MR angiogram (Fig 4B) but poorly seen on the delayed DSA images (Fig 4G).

Postoperative MR studies were obtained in four cases—patients 5, 6, and 7 at 3 to 4 months and patient 2 at 6 months after surgery. The MR angiography findings (Fig 2G) indicated that the dural fistula had been obliterated in all four cases. In patient 7, obliteration of the right T-8 fistula was confirmed by DSA. All patients improved clinically. On T2-weighted images, there was a marked decrease in the extent of cord hyperintensity (Fig 2F), whereas on postgadolinium T1-weighted images there were varying degrees of residual cord enhancement.

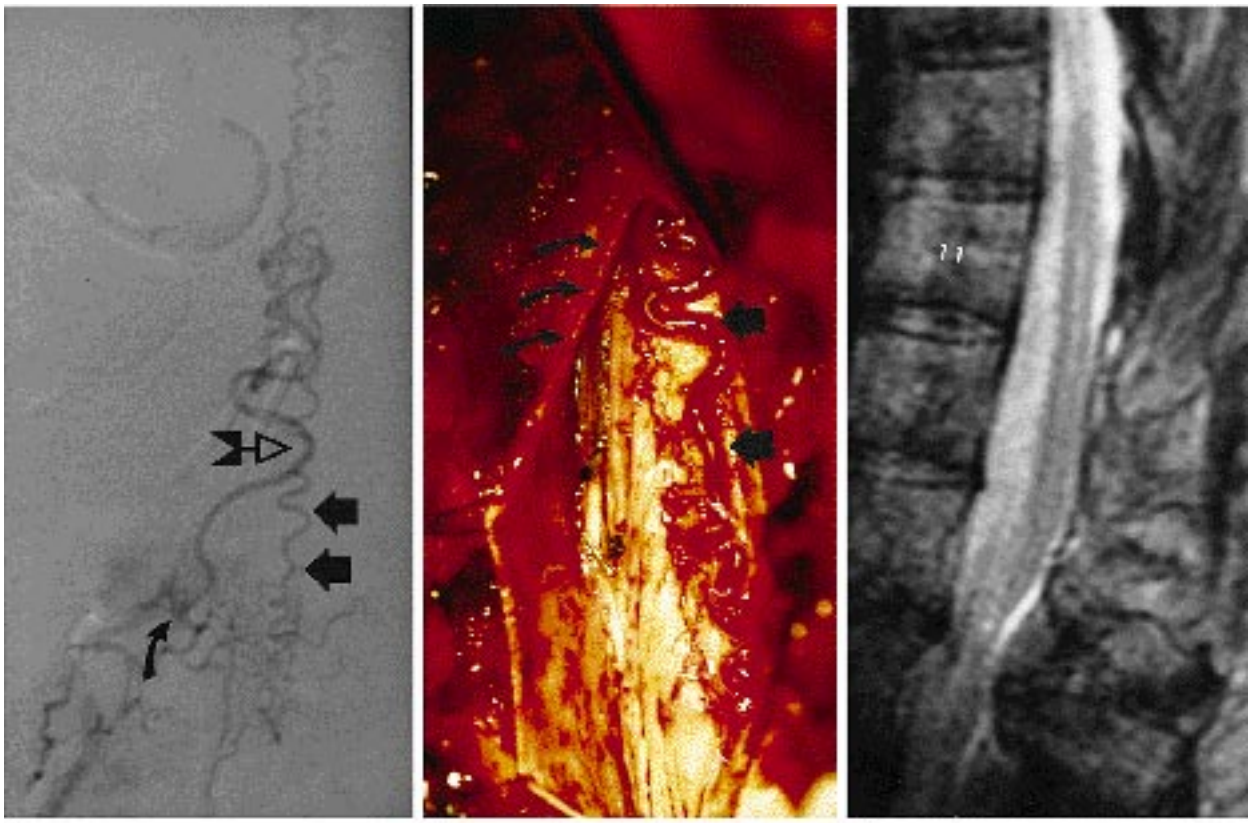

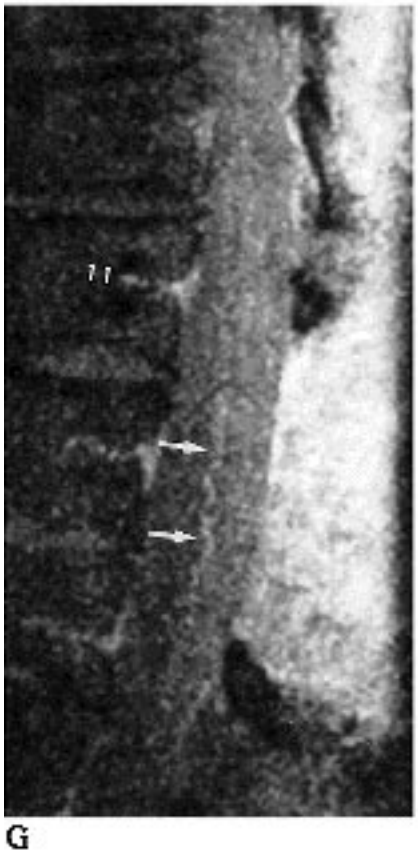

Fig 2, *continued.*

D, DSA left anterior oblique view, obtained 15 seconds after injection of the right T-12 intercostal artery. The medullary vein draining from the fistula (*curved arrow*) in the right T-12 foramen has a midline segment (*open arrow*) and tortuous course before anastomosing with the coronal venous plexus. This T-12 medullary vein corresponds to the vessel described in C. The same question mark configuration (*arrows*) of the posterior median vein at T-12 is demonstrated.

E, Intraoperative photograph of the posterior surface of the cord. The right and left sides of the original photographic image have been reversed to display the patient's right side on the reader's left. The question mark configuration (*arrows*) of the posterior median vein is identified. The right T-12 medullary vein is obscured by partially reflected dura (*curved arrows*).

F, Postoperative, sagittal T2-weighted image demonstrates resolution of the cord hyperintensity shown in A.

G, Postoperative, postgadolinium, midsagittal MR angiogram (T-9 to L-2) shows a minimally serpiginous vessel along the anterior surface of the cord (*arrows*), corresponding to the anterior median vein. The engorgement and tortuosity of the intradural veins demonstrated in B are no longer observed. (The medullary vein identified in C exhibited no enhancement and was not visible on the postoperative source images.) Scar tissue within the laminectomy defect at T-12 enhances with gadolinium.

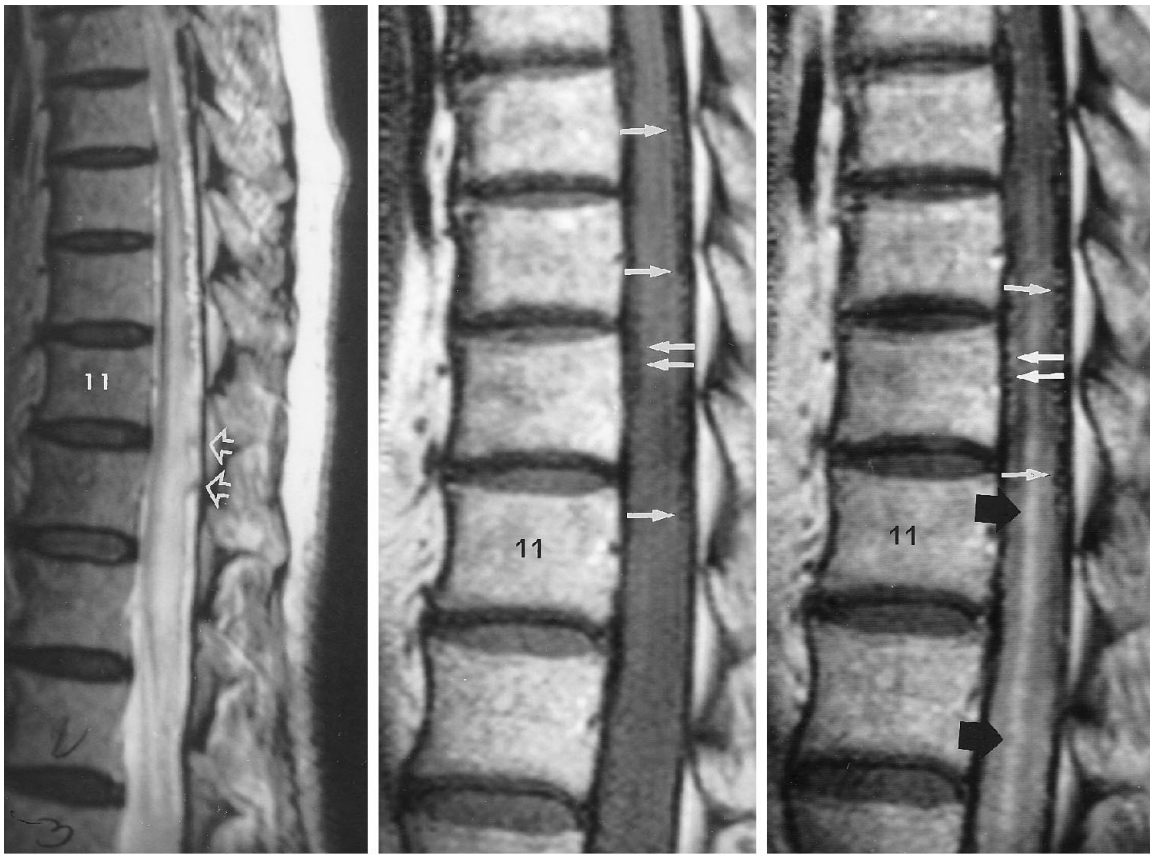

Fig 3. Right T-12 dural AVF (patient 8).

A, Midsagittal, T2-weighted, fast spin-echo image demonstrates hyperintensity within the lower thoracic cord. The cerebrospinal fluid signal in the subarachnoid space posterior to the cord from T-9 to T-11 appears serrated, with a focal hypointensities (*open arrows*) posteriorly at T-12.

B, Pregadolinium and *C*, postgadolinium T1-weighted images show the scalloped contour of the anterior and posterior surfaces (*white arrows*) of the lower thoracic cord attributable to enlarged vessels. Some vessel segments show enhancement in C. The cord enhances, especially centrally (*arrows*), between T-9 and L-2, with enlargement of the conus. *Figure continues.*

Discussion

Spinal vascular anatomy

To interpret the results of postgadolinium MR angiography of the spine, a knowledge of spinal vascular anatomy, with emphasis on the intradural veins which are extrinsic to the cord, is important. A review of normal anatomy is beyond the intent of this paper (but can be found elsewhere [23–25]); however, some salient features are described below.

The venous drainage of the spinal cord does not parallel the arterial supply (26–28). Like the extrinsic arterial system, the extrinsic venous system has two parts: (*a*) longitudinal trunks, and (*b*) a pial plexus, termed the *coronal venous plexus*. The main arterial supply, anterior spinal artery, is on the anterior surface of the cord, whereas the major venous channel is on the posterior surface, the posterior median vein (PMV). This longitudinal trunk vein has a midline location, whereas the relatively small posterior arterial trunks are off midline (eg, posterolateral). According to Thron and others, the PMV and the corresponding anterior median vein (AMV) are the largest vessels on the cord, and in the thoracolumbar region, they range from 0.8 to 1.5 mm in postmortem, contrast-injected specimens (23, 25, 28). The PMV is usually the larger vessel (for example, Fig 1), as much as 2.5 times the size of the AMV (26, 28). The AMV parallels the anterior spinal artery (0.5 to 0.8 mm maximum diameter [23]), lying slightly deeper and to the side of the artery in the median sulcus. Thus, an anterior median vessel identified on MR angiography can repre-

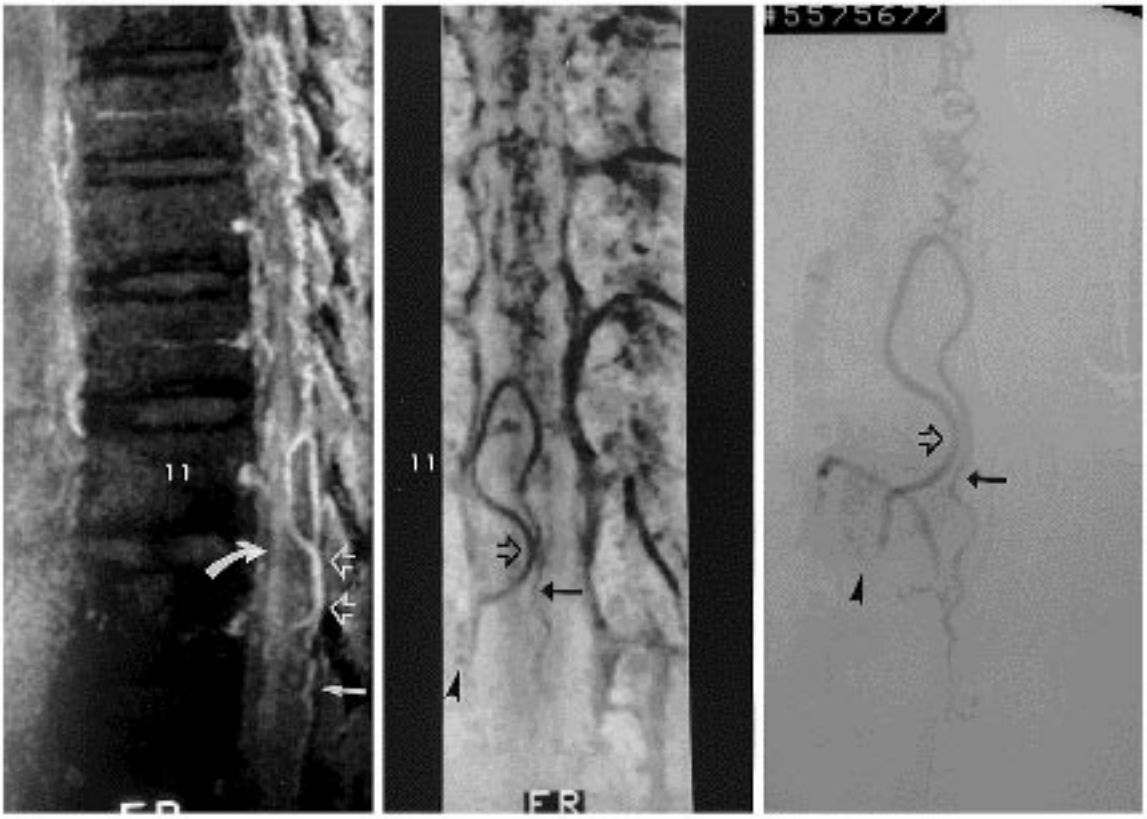

D E F

G H

sent either the AMV or the anterior spinal artery. It may be possible to distinguish between the two vessels in the thoracolumbar region, because the anterior spinal artery anatomoses with the posterolateral arteries at the tip of the conus, whereas the AMV usually continues caudally (Fig 4B) as a very large terminal vein, accompanying the filum terminale to the end of the dural sac (27).

In our study, the term *medullary veins* refers to the veins that accompany some of the spinal nerve roots and drain blood from the AMV, the PMV, and the coronal venous plexus on the cord surface to the epidural venous plexus. In the thoracolumbar region, there is usually just one large anterior and one or two large ("great") posterior medullary veins, measuring up to 1.5 mm, accompanying lower thoracic or upper lumbar roots (27, 29). The medullary veins, as described by Gillilan and other (13, 20, 27), correspond to *les veines radiculaires* described by French anatomists (24). In Figure 1C, the posteriorly located vessel coursing inferolaterally from the midline toward the right T-12 neural foramen corresponds in location to the great posterior medullary vein. It is unlikely to be an artery , because there is no great posterior medullary artery extending to the midline in the thoracolumbar region (25).

Based on the results of the previous postcontrast MR angiography studies (22, 30, 31), it is expected that our technique would improve visibility of small spinal intradural vessels, especially veins. Our use of longer echo times, usually 10 milliseconds, also might contribute to visibility of the spinal veins more than arteries, because signal loss resulting from intravoxel dephasing usually affects arteries and is worse at longer echo times (32). The primary reason the intradural vessels detected on postgadolinium MR angiography in healthy subjects are likely to be veins is that the extrinsic veins are much larger than the extrinsic arteries, as discussed above. Thus, it should not be surprising that the intradural vessels depicted in Figure 1 correspond to the AMV and PMV and the great posterior medullary vein draining to the right T-12 neural foramen. In cases of AVF, the disparity in size between the intradural veins draining the fistula and spinal arteries is even greater, further improving conspicuity of these veins, other factors being equal.

Spinal Vascular Malformations: Dural AVF

Based in large part on work by Djindjian (11, 33); Kendall, Logue, and colleagues (16, 20); Merland et al (12, 34); and Doppman, DiChiro, and colleagues (13, 15, 35), the classification of spinal vascular malformations is divided into two main categories: intradural and dural. Intradural lesions may be further subcategorized into intramedullary and extramedullary AVMs or AVFs (13, 14, 36). Dural lesions are called *fistulas* by some (34) and *malformations* by others (16, 20). The former term is commonly used in angiographic descriptions (13). In the recent classification proposed by Anson and Spetzler (14), there are four types of spinal AVMs: type 1 is a dural AVF; type 2 is an intramedullary glomus-type AVM; type 3 is an intramedullary juvenile-type AVM, which frequently has an extramedullary component and sometimes an extradural component; and type 4 is an intradural, extramedullary AVF. Type 1

Fig 3, *continued*.

D, Postgadolinium, subvolume MR angiogram (T-7 to L-1) encompassing the right half of the canal. A single large vessel courses posteriorly from the region of the right T-12 foramen to reach the posterior surface of the cord at T11–12 (*open arrows*). The vessel continues anteriorly and superiorly along the right side of the cord at T-11 before turning posteriorly to anastomose with the vessels on the posterior surface of the cord. From T-10 to T7–8, these vessels are highly convoluted. Below the level of the fistula, a single posterior median vessel (*large arrow*) is observed. The enhancement within the cord (*curved arrow*) is distinguishable from the extramedullary, intradural vessel enhancement.

E, Coronal, subvolume MR angiogram (inverted gray scale) from the same acquisition as D. The large vessel described in D follows an S-shaped course from the right T-12 neural foramen (*arrowhead*) to the midline (*open arrow*), then superiorly along the right side of the cord to reach the midline anastomosis at T10–11. As in D, convoluted vessels are present above the anastomosis, whereas below it, a single midline vessel (*arrow*) is observed.

F and *G*, DSA posteroanterior views, obtained 17 seconds (F) and 12 seconds (G) after injection of the dorsal ramus of the right T-12 intercostal artery. The course of the medullary vein draining the fistula is the same as that shown on the MIP images (D and E). At T11–12, the midline segment (*open arrow*) of the medullary vein parallels the posterior median vein (*arrow*) draining inferiorly. Above the anastomosis at T10–11, there are convoluted veins that correspond to the vessels demonstrated by MR angiography in E. The dural fistula (*arrowhead*) at T-12 is better shown in the earlier postinjection image (G).

H, Intraoperative photograph of the posterior surface of the cord. The patient's right side is on the reader's left, as in Figure 2E. The medullary vein (*open arrow*) is "arterialized." It is adjacent to the posterior median vein (*arrow*), as demonstrated in E, F, and G.

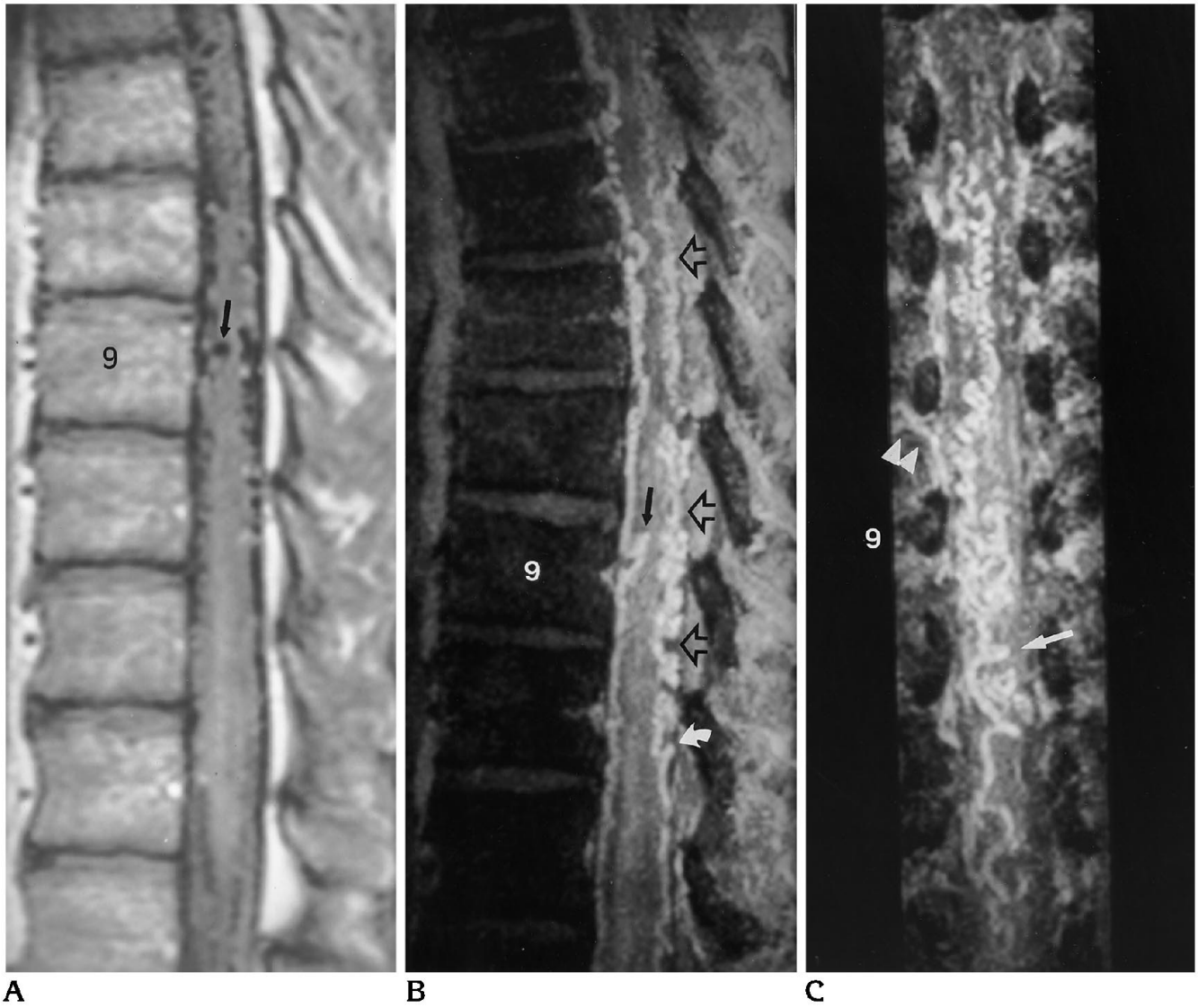

Fig 4. Right T-8 dural AVF (patient 7).

A, Postgadolinium, midsagittal, T1-weighted image. The anterior and posterior surfaces of the cord have scalloped contours attributable to hypointense areas caused by engorged intradural vessels. At T-9 anteriorly, a vascular "flow void" (*arrow*) appears to be intramedullary. The scalloping decreases caudally and is not seen at the conus tip (T12-L1). Enhancement and enlargement of the cord primarily involve the conus.

B, Postgadolinium, midsagittal, subvolume MR angiogram (T-4 to T-12). Numerous convolutions of intradural vessels (*open arrows*) are seen along the posterior surface of the cord, although only one large vessel (*curved arrow*) is apparent inferiorly. A relatively enlarged vessel along the anterior surface of the cord represents an engorged anterior median vein (see G), with a kink (*arrow*) at T-9 corresponding to the apparent intramedullary vessel in A. On a second overlapping slab acquisition, the vessel(s) along the anterior surface of the cord were demonstrated to the level of C-6. Compare the appearance of the anterior median vein from T-9 to T-12 with that of the anterior vein in the healthy subject (Fig 1B).

C, Coronal subvolume MR angiogram, from the same acquisition as B. The subvolume includes only the posterior half of the canal and demonstrates the posterior coronal venous plexus. From T-10 to T-12, the dominant, tortuous posterior median vein is seen, and a "reverse 7" segment (*arrow*) is identified. In the right T-8 foramen, two vessel segments are seen. The more inferior segment (*arrowheads*) appears to traverse the foramen—a finding not demonstrated at other spinal levels—and approximates the location of the feeding artery to the fistula, as shown in D. *Figure continues.*

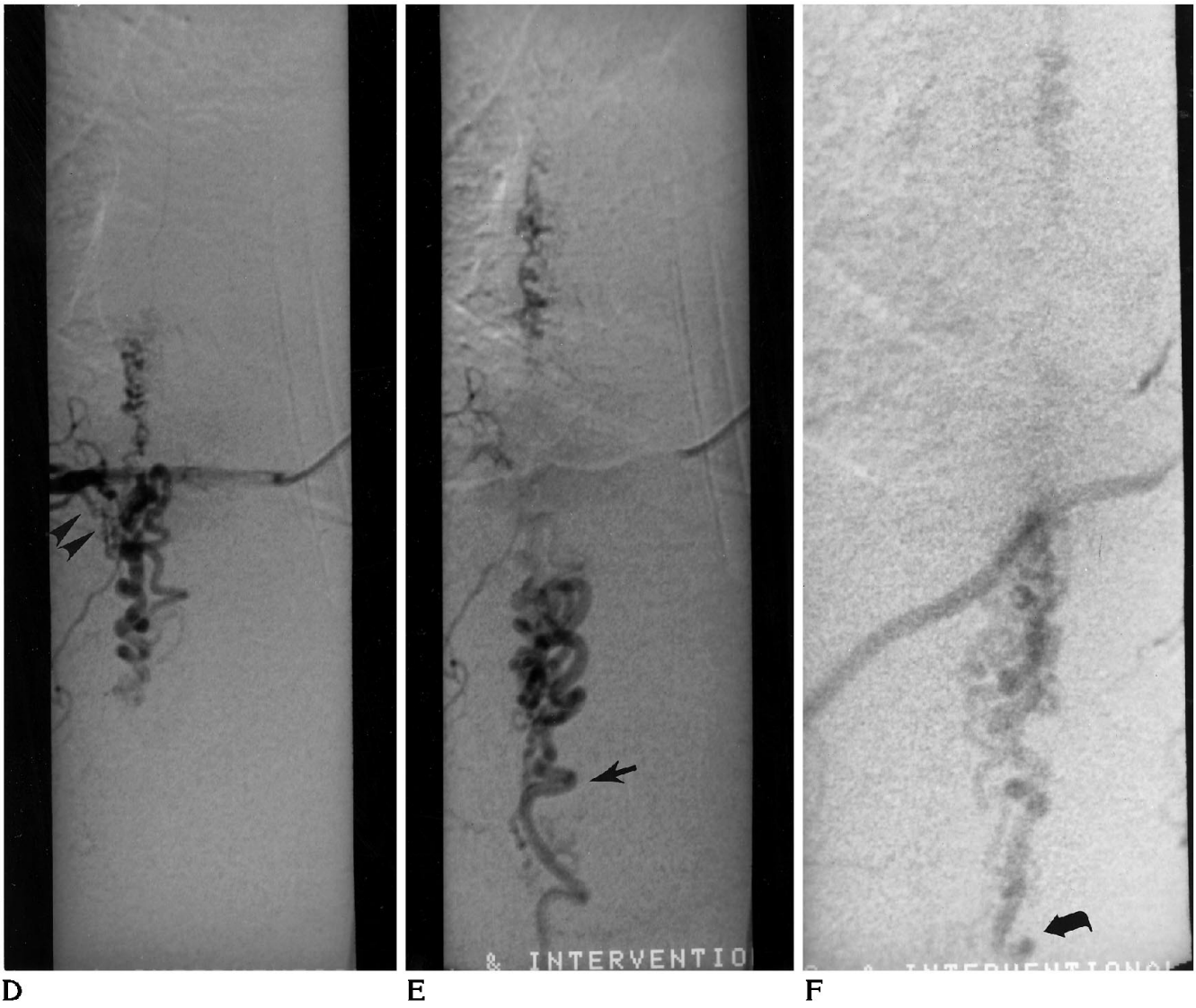

Fig 4, *continued.*

D and *E*, DSA posteroanterior view, obtained at 6 seconds (D) and 9 seconds (E) after injection of the right T-8 intercostal artery. The fistula (*arrowheads*) and early draining intradural veins are demonstrated. In the later image, additional intradural veins are visible, whereas the veins opacified initially are no longer seen because of wash-out of contrast material. The reverse 7 segment (*arrow*) of the posterior median vein is seen in E, but not in D.

F and *G*, DSA lateral view, obtained at 10.5 seconds (F) and 18.5 seconds (G) after injection of the right T-8 intercostal artery. In F, only the posterior coronal venous plexus at T-9 and T-10 is opacified. Comparison between the angiographic image (F) and the midsagittal MR angiogram (B) reveals a similar contour (*curved arrow*) of the posterior median vein at T-10; however, most of the anterior and posterior coronal veins shown in B are not displayed in F. *Figure continues.*

dural AVFs are subcategorized as type 1A (single feeding artery) and type 1B (multiple feeding arteries).

Dural AVFs are considered acquired lesions, which almost always appear in the thoracolumbar spine (13). On conventional angiography, type 1 dural AVF consists of a vascular nidus or shunt supplied by the dural branch of the radiculomedullary-dural artery (36). The nidus, located in the region of the neural foramen, is drained intradurally by retrograde flow through the medullary vein, resulting in engorgement of the coronal venous plexus and the intraparenchymal radial veins (13, 16). Rosenblum et al (13) reported that rapid blood flow, defined as an angiographic arterial

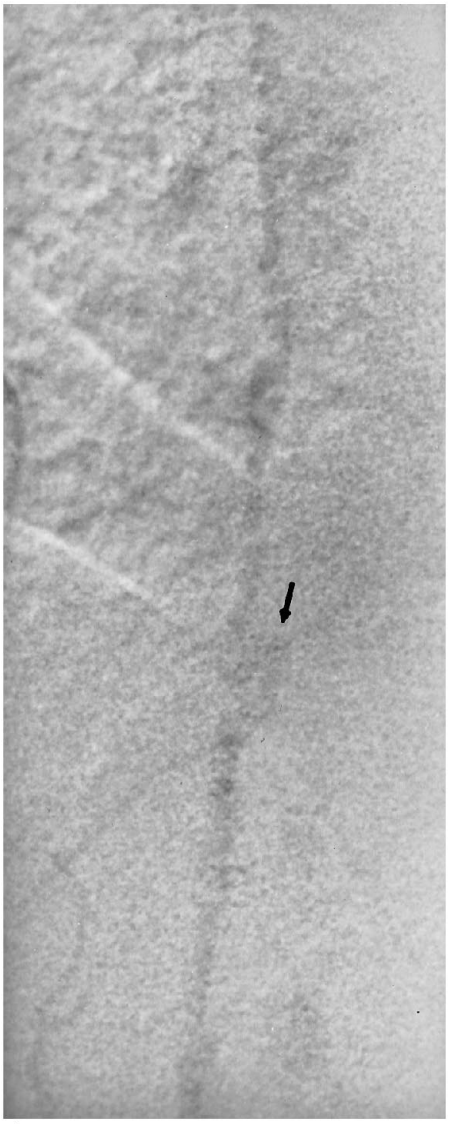

G

Fig 4, *continued.*

G, In this later image, the anterior median vein is opacified, yet contrast is poor. The "kink" (*arrow*) at T-9 is marginally visible.

phase lasting less than 6 seconds, did not occur with dural AVFs.

Clinically, dural AVFs more commonly affect male subjects and present with gradual onset and progressive, sometimes fluctuating, deterioration of neurologic function. This is most commonly manifested as spastic paresis of the lower extremities and loss of sensation of pain and temperature (16). Usually a distinct sensory level is present, reflecting the level of the fistula (13). All eight of the patients with dural AVF examined during this study had clinical findings consistent with this picture of progressive myelopathy. Although the combination of upper and lower motor neuron deficits is suggestive, it is not specific, and patients with intramedullary tumor, myelitis, or cord compression from any cause may have a similar initial presentation (16, 37).

Several published studies (6–9) have described the MR imaging findings in cases of dural AVF: slight enlargement of the lower spinal cord; cord hypointensity of T1-weighted images and hyperintensity on T2-weighted images involving the central region of the cord and extending over several levels; scalloping of the cord contours on sagittal images; serpiginous areas of low signal intensity ("flow void") on T2-weighted images; and enhancement of the cord on T1-weighted images after intravenous administration of gadopentetate dimeglumine. Among these findings, the one that has been observed consistently is hyperintensity within the center of the cord on T2-weighted images. A recent review by Mayo Clinic researchers of 91 spinal vascular malformations, including 62 dural AVFs, revealed that the only MR finding that was present in all cases was cord hyperintensity on T2-weighted images (Gilbertson JR et al, "Spinal Dural Arteriovenous Fistulae: A Comprehensive Analysis of MR and Myelographic Findings," presented at the 32nd Annual Meeting of the American Society of Neuroradiology, Nashville, Tenn, May 3–7, 1994). In a study of 11 patients with dural AVF, Tewey et al (9) obtained postgadolinium T1-weighted images in 5 and found that delayed (40 to 45 minutes), but not immediate, cord enhancement after injection was present in each subject. In our study, we also found that there was increased signal intensity within the cord on T2-weighted images and cord enhancement on T1-weighted images in all subjects, whereas observation of cord enlargement and decreased cord signal on T1-weighted images was not uniformly present. The average extent of the hyperintense signal on T2-weighted images was 5 vertebral levels, being predominantly cephalad to the T-12 fistulas (n = 4), caudal to the T-5 (n = 1) and T-8 (n = 2) fistulas, and centered about the T-10 (n = 1) fistula.

The additional MR finding of flow-related signal abnormalities in the subarachnoid space is crucial to diagnostic accuracy, yet is not always present (Gilbertson JR et al, "Spinal Dural Arteriovenous Fistulae," 1994). Terwey et al (9)

reported this finding in only 7 of their 11 cases of dural AVF. Although Minami et al (7) found scalloping of the posterior surface of the cord on T1-weighted images, attributable to vessels, in all of their 6 cases, the scalloping was described as "minute" in 2. Nevertheless, these authors considered this finding more reliable than identification of serpiginous low signal on T2-weighted images, which could be obscured by cerebrospinal fluid pulsation artifacts. We found dotlike or serpiginous signal abnormality in the subarachnoid space on spin-echo images in the majority, but not all, of the subjects with dural AVF (Table), in agreement with previous authors. Identification of intravascular flow-induced signal loss at one or two levels (Fig 2A) may not be sufficiently convincing to diagnose spinal AVM or recommend catheter angiography. Because conspicuity of abnormal vessels on spin-echo images may depend on flow-velocity (38), imaging parameters such as spatial resolution and motion compensation, bulk motion artifacts, and general quality of the examination, it has been said that a negative MR imaging study does not rule out spinal AVM (37). Thus, in cases with convincing clinical evidence of dural AVF and negative or equivocal MR findings, myelography has been recommended by some authors for detection of dilated and tortuous intradural vessels (23, 39). The classic myelographic appearance of these vessels as serpiginous filling defects, though, may be seen in other conditions such as tumor, arachnoiditis, and redundant nerve roots (40). Also, myelography may be normal in patients with spinal AVM (39, 40). Djindjian (41) found that 10% of 105 cases of spinal AVM were normal, whereas 46% had characteristic serpiginous filling defects on myelography.

In the detection and identification of intravascular flow-related signal in the subarachnoid space, it is apparent from Figures 2 and 3 that MR angiography is superior to spin-echo MR imaging. Figure 2 is an example of cases, such as those described by Terwey et al (9), in which abnormal cord signal and enhancement are observed, yet evidence of abnormal vessels in the subarachnoid space is marginal. In these cases, MR angiography provides the additional screening information that potentially can improve the diagnostic accuracy of MR. As shown in Figures 2, 3, and 4, the abnormal vessels represent the engorged veins of the coronal venous plexus and particularly the AMV and PMV. Because blood flow in the extrinsic veins draining the dural fistula can be relatively slow compared with the rapid flow occurring with intradural AVMs (13), and because spin satuation is likely to be appreciable given the coronal or sagittal orientation of the 3-D slab, postgadolinium studies markedly improve depiction of these veins. MR angiography provides information about their relative size, number, and tortuosity—information that was previously obtained from myelography.

With our technique, pregadolinium MR angiography did not show intradural vessels in healthy subjects (Fig 1A) and only occasionally demonstrated segments of abnormal vessels near the fistula site in patients with dural AVF. Thus, for screening purposes generally, the pregadolinium 3-D slab acquisition can probably be omitted; however, in cases of suspected hemorrhage or thrombosis of spinal vessels, and in postoperative or postembolization evaluation (see below), the pregadolinium acquisition should be retained to clarify questions of hyperintense signal not obviously attributable to flowing blood. Review of the source images from postgadolinium, as well as pregadolinium, slab acquisitions is necessary, not only in these cases but in all MR angiography screening studies. The intradural vessels are distinguished from the epidural plexus on the source images, thus guiding placement of the region of interest for targeted MIP images. On technically adequate studies, the source plus MIP images almost always allowed differentiation of tortuous intradural veins from the epidural plexus.

By demonstrating a dominant, tortuous medullary vein, postgadolinium MR angiography provides valuable screening information for dural fistula beyond the improved depiction of abnormal intradural vessels compared with MR imaging. First, knowing the course of the medullary vein (Fig 2C and 3E), one may suggest the location of a suspected fistula, thus directing the DSA study to certain spinal levels initially and potentially shortening the overall time of the study. As shown in the Table, a dominant medullary vein was identified on MR angiography in 6 of the 8 cases of dural fistula, and conspicuous foraminal vessels were identified in an additional case. Second, by reviewing both the coronal and sagittal projection angiograms and source images, one can determine whether the initial drainage is anterior or poste-

rior to the cord. Determining these locations may be difficult on conventional angiography limited to posteroanterior and oblique views, yet is important to the surgeon.

Because MR angiography does not have the temporal resolution of DSA, more enlarged veins may be seen on the MIP images that on individual frames of the DSA filming sequence. For example, in patient 7, the midline, subvolume MR angiogram (Fig 4B) shows enlarged vessels posterior and anterior to the cord (Table), whereas DSA first shows the posterior coronal venous plexus and later the anterior median vein (Fig 4D–G). The AMV is better shown by MR angiography than by DSA, probably because with DSA there is contrast dilution and patient motion on the delayed frames. The improved visibility of more slowly draining veins on MR angiography make this technique complementary to DSA, which has unparalled sensitivity in demonstrating spinal arteries in vivo.

Postoperative MR Angiography

Two approaches to the treatment of type 1 dural AVF have been advocated (14). In the first approach, the dural nidus is removed surgically, and the feeding artery and draining vein are clipped, without resection or "stripping" of the engorged coronal venous plexus (35). This was the approach used to treat six AVF (patients 3 through 8, Table) in our series. Postoperative MR angiography was obtained in three (patients 5, 6, and 7) and DSA in one (patient 7), at 3 to 4 months after surgery. In patients 5 and 6, MR angiography showed one or a few nonenlarged, minimally serpiginous vessels (Fig 2G) along the cord, whereas the abnormal medullary vein draining the fistula before surgery was no longer seen. In patient 7, the enlarged veins of the posterior coronal plexus were no longer seen on MR angiography. The anterior median vein was still seen; however, it was decreased in size and tortuosity. The prominent foraminal vessels on the right at T-8 were no longer demonstrated, and DSA confirmed obliteration of the fistula. Thus, MR angiography provided evidence noninvasively that these fistulas had been obliterated. This evidence was in agreement with findings of clinical improvement and near resolution of cord hypertensity of T2-weighted MR imaging (Fig 2F).

In the other approach to treatment of dural AVF, endovascular therapy is advocated as the primary modality, with surgery reserved for patients in whom embolization has failed (10, 12). Embolization of dural fistula with polyvinyl alcohol has been problematic because of the high rate of delayed recanalization (42). Patient 2 in our series was initially treated by embolization with polyvinyl alcohol, and MR angiography showed no change in the appearance of the dominant medullary vein at 1 month and at 5 months after embolization. After surgical removal of the fistula, the vein was no longer seen. Thus, MR angiography could be used to monitor both unsuccessful and successful treatment of the fistula. Embolization of spinal AVMs also has been accomplished using cyanoacrylate "glue." Recanalization is not a problem with this agent; however, none of the subjects in our series were treated with it.

Conclusion

The results obtained from this study indicate that postgadolinium MR angiography can provide valuable information in screening for dural AVF (type 1 spinal AVM [14]). MR angiography (*a*) provides delineation of abnormal intradural vessels, when evidence of abnormal vessels on spin-echo images is subtle or absent; (*b*) demonstrates a dominant medullary vein and its corresponding foraminal level and, therefore, has value in determining the level of the fistula and its feeding artery; and (*c*) can be used as a noninvasive technique for monitoring the success of treatment.

Acknowledgments

We thank Kathe Holmes for technical assistance with MR angiography, Lisa Kornse and Sherri Patchen for coordinating all aspects of patient care, and Jean Alli for assistance in the preparation of the manuscript.

References

1. Bowen BC, Quencer RM, Margosian P, Pattany PM. MR angiography of occlusive disease of the arteries in the head and neck: current concepts. *AJR Am J Roentgenol* 1994;162:9–18
2. Gelbert F, Guichard J-P, Mourier KL, et al. Phase-contrast MR angiography of vascular malformations of the spinal cord at 0.5T. *J Magn Reson Imaging* 1992;2:631–636
3. Turski PA, Korosec FR, Graves VB, Strother CM. Vascular malformations. In: Potchen EJ, Haake ME, Siebert JE, Gottschalk A, eds. *Magnetic Resonance Angiography: Concepts and Applications.* St Louis: Mosby, 1993:380–404

4. Friedman DP, Flanders AE, Tartaglino LM. Vascular neoplasms and malformations, ischemia and hemorrhage affecting the spinal cord: MR imaging findings. *AJR Am J Roentgenol* 1994;162:685–692
5. Provenzale JM, Tien RD, Felsberg GJ, Hacein-Bey L. Spinal dural arteriovenous fistula: demonstration using phase contrast MRA. *J Comput Assist Tomogr* 1994;18:811–814
6. Masaryk TJ, Ross JR, Modic MT, et al. Radiculomeningeal vascular malformations of the spine: MR imaging. *Radiology* 1987;164: 845–849
7. Minami S, Sagoh T, Nishimura K, et al. Spinal arteriovenous malformation: MR imaging. *Radiology* 1988;169:109–115
8. Dormont D, Gelbert F, Assouline E, et al. MR imaging of spinal arteriovenous malformations at 0.5T: study of 34 cases. *AJNR Am J Neuroradiol* 1988;9:833–838
9. Terwey B, Becker H, Thron AK, Vahldiek G. Gadolinium-DTPA enhanced MR imaging of spinal dural arteriovenous fistulas. *J Comput Assist Tomogr* 1989;13:30–37
10. Choi IS, Berenstein A. Surgical neuroangiography of the spine and spinal cord. *Radiol Clin North Am* 1988;26:1131–1141
11. Djindjian M, Djindjian R, Rey A, et al. Intradural extramedullary spinal arteriovenous malformations fed by the anterior spinal artery. *Surg Neurol* 1977;8:85–93
12. Merland JJ, Reizine D. Treatment of arteriovenous spinal cord malformations. *Semin Intervent Radiol* 1987;4:281–290
13. Rosenblum B, Oldfield EH, Doppman JL, DiChiro G. Spinal arteriovenous malformations: a comparison of dural arteriovenous fistulas and intradural AVM's in 81 patients. *J Neurosurg* 1987; 67:795–802
14. Anson JA, Spetzler RF. Spinal dural arteriovenous malformations. In: Awad IA, Barrow DL, eds. *Dural Arteriovenous Malformations*. Park Ridge, Ill: American Association of Neurological Surgeons, 1993:175–191
15. Ommaya AK, DiChiro, Doppman J. Ligation of arterial supply in the treatment of spinal cord arteriovenous malformations. *J Neurosurg* 1969;30:679–692
16. Symon L, Kuyama H, Kendall B. Dural arteriovenous malformations of the spine: clinical features and surgical results in 55 cases. *J Neurosurg* 1984;60:238–247
17. Doppman JL, DiChiro G, Ommaya AK. Percutaneous embolization of spinal cord arteriovenous malformations. *J Neurosurg* 1971;34:48–55
18. Halbach VV, Higashida RT, Dowd CF, et al. Treatment of giant intradural (perimedullary) arteriovenous fistulas. *Neurosurgery* 1993;33:972–980
19. Aminoff MJ, Logue V. Clinical features of spinal vascular malformations. *Brain* 1974;97:197–210
20. Kendall BE, Logue V. Spinal epidural angiomatous malformations draining into intrathecal veins. *Neuroradiology* 1977;13:181–189
21. Prince MR. Gadolinium-enhanced MR aortography. *Radiology* 1994;191:155–164
22. Sze G, Goldberg SN, Kawamura Y. Comparison of bolus and constant infusion methods of gadolinium administration in MR angiography. *AJNR Am J Neuroradiol* 1994;15:909–912
23. Thron, AK. *Vascular Anatomy of the Spinal Cord: Neuroradiological Investigations and Clinical Syndromes*. New York, NY: Springer-Verlag, 1988;7:13–64
24. Moes P, Maillot CI. Les veines superficielles de la moelle epiniere chez l'homme: essai de systematisation. *Arch Anat Histol Embryol* 1981;64:5–110
25. Lasjaunias P, Berenstein A. *Surgical Neuroangiography, III: Functional Vascular Anatomy of Brain, Spinal Cord and Spine*. New York, NY: Springer-Verlag, 1990:15–87
26. Suh TH, Alexander L. Vascular system of the human spinal cord. *Arch Neurol Psychiatr* 1939;41:659–677
27. Gillilan LA. Veins of the spinal cord: anatomic details; suggested clinical applications. *Neurology* 1970;20:860–868
28. Fried LC, Doppman JL, DiChiro G. Venous phase in spinal cord angiography. *Acta Radiol* 1971;11:393–401
29. Jellinger K. *Zur Orthologie und Pathologie der Ruckenmarksdurchblutung*. New York, NY: Springer-Verlag, 1966
30. Chakeres DW, Schmalbrock P, Brogan M, et al. Normal venous anatomy of the brain: demonstration with gadopentetate dimeglumine in enhanced 3-D MR angiography. *AJR Am J Roentgenol* 1991;156:161–172
31. Creasy JL, Price RR, Presbrey T, et al. Gadolinium-enhanced MR angiography. *Radiology* 1990;175:280–283
32. Schmalbrock P, Yuan C, Chakeres DW, et al. Volume MR angiography: methods to achieve very short echo times. *Radiology* 1990;175:861–865
33. Hurth M, Houdart R, Djindjian R, et al. Arteriovenous malformations of the spinal cord. *Prog Neurol Surg* 1978;9:238–266
34. Merland JJ, Riche MC, Chiras J. Intraspinal extramedullary arteriovenous fistula draining into the medullary veins. *J Neuroradiol* 1980;7:271–320
35. Oldfield EH, DiChiro G, Quindlen EA, et al. Successful treatment of a group of spinal cord arteriovenous malformations by interruption of dural fistula. *J Neurosurg* 1983;59:1019–1030
36. Enzmann DR. Vascular diseases. In: Enzmann DR, LaPaz RL, Rubin JB, eds. *Magnetic Resonance of the Spine*. Baltimore, Md: Mosby Company, 1990:510–539
37. Rosenblum DS, Myers SJ. Dural spinal cord arteriovenous malformation. *Arch Phys Med Rehabil* 1991;72:233–236
38. Doppman JL, DiChiro G, Dwyer AJ, et al. Magnetic resonance imaging of spinal arteriovenous malformations. *J Neurosurg* 1987;66:830–834
39. Gulliver D, Noakes J. Myelographic differentiation of spinal cord arteriovenous malformations from the normal population. *Australas Radiol* 1988;32:57–64
40. Tobin WD, Layton DD. The diagnosis and natural history of spinal cord arteriovenous malformations. *Mayo Clin Proc* 1976;51:637–646
41. Djindjian R. Vascular malformations. In: Shapiro R, ed. *Myelography*. 4th ed. Chicago, Ill: Year Book Publishers, 1984:318–344
42. Morgan MK, Marsh WR. Management of spinal dural arteriovenous malformations. *J Neurosurg* 1989;70:832–836